Response of the medial temporal lobe network in amnestic mild cognitive impairment to therapeutic intervention assessed by fMRI and memory task performance

CrossMark

Arnold Bakker[a],[*], Marilyn S. Albert[b], Gregory Krauss[b], Caroline L. Speck[a], Michela Gallagher[c]

[a]Department of Psychiatry and Behavioral Sciences, Johns Hopkins University School of Medicine, Baltimore, MD 21287, USA
[b]Department of Neurology, Johns Hopkins University School of Medicine, Baltimore, MD 21287, USA
[c]Department of Psychological and Brain Sciences, Johns Hopkins School of Arts and Sciences, Baltimore, MD 21218, USA

ARTICLE INFO

ABSTRACT

Studies of individuals with amnestic mild cognitive impairment (aMCI) have detected hyperactivity in the hippocampus during task-related functional magnetic resonance imaging (fMRI). Such elevated activation has been localized to the hippocampal dentate gyrus/CA3 (DG/CA3) during performance of a task designed to detect the computational contributions of those hippocampal circuits to episodic memory. The current investigation was conducted to test the hypothesis that greater hippocampal activation in aMCI represents a dysfunctional shift in the normal computational balance of the DG/CA3 regions, augmenting CA3-driven pattern completion at the expense of pattern separation mediated by the dentate gyrus. We tested this hypothesis using an intervention based on animal research demonstrating a beneficial effect on cognition by reducing excess hippocampal neural activity with low doses of the atypical anti-epileptic levetiracetam. In a within-subject design we assessed the effects of levetiracetam in three cohorts of aMCI participants, each receiving a different dose of levetiracetam. Elevated activation in the DG/CA3 region, together with impaired task performance, was detected in each aMCI cohort relative to an aged control group. We observed significant improvement in memory task performance under drug treatment relative to placebo in the aMCI cohorts at the 62.5 and 125 mg BID doses of levetiracetam. Drug treatment in those cohorts increased accuracy dependent on pattern separation processes and reduced errors attributable to an over-riding effect of pattern completion while normalizing fMRI activation in the DG/CA3 and entorhinal cortex. Similar to findings in animal studies, higher dosing at 250 mg BID had no significant benefit on either task performance or fMRI activation. Consistent with predictions based on the computational functions of the DG/CA3 elucidated in basic animal research, these data support a dysfunctional encoding mechanism detected by fMRI in individuals with aMCI and therapeutic intervention using fMRI to detect target engagement in response to treatment.

1. Introduction

A longstanding computational theory attributes successful memory to a balance between two complementary functions mediated by the hippocampal dentate gyrus and CA3 regions, which receive input from layer II neurons of the entorhinal cortex. The model proposes that pattern separation, a function ascribed to the granule cells of the dentate gyrus, reduces mnemonic interference by encoding distinctive representations for similar input patterns, while pattern completion refers to the recovery of a prior representation from partial or degraded input, a function ascribed to the extensive recurrent collaterals of CA3 neurons (McClelland et al., 1995; Norman and O'Reilly, 2003; O'Reilly and McClelland, 1994; Treves and Rolls, 1994); for a review see Yassa and Stark (2011). It has been proposed that such competing, yet complementary processes would minimize interference while maximizing storage capacity for episodic memories. Empirical evidence consistent with this model is supported by studies of the encoding properties of neurons in these brain regions in laboratory animals (Alme et al., 2014; Lee et al., 2004; Leutgeb et al., 2004; Neunuebel and Knierim, 2014). High-resolution functional magnetic resonance imaging (fMRI) has also demonstrated alterations in fMRI activation in the DG/CA3 regions consistent with such computational functions in the human brain (Bakker et al., 2008; Yassa et al., 2010, 2011a).

In elderly human subjects (compared to young adults) and in patients with aMCI (compared to age-matched controls), increased fMRI

* Corresponding author at: Department of Psychiatry and Behavioral Sciences, Johns Hopkins University School of Medicine, 600 N. Wolfe Street/Phipps 300, Baltimore, MD 21287, USA. Tel.: +1 410 502 6944; fax: +1 410 614 3676.
E-mail address: abakker@jhu.edu (A. Bakker).

BOLD activation was localized to the DG/CA3 region (Yassa et al., 2010, 2011a), using a three-judgment memory task designed to tax pattern separation. In both cases, increased activity was correlated with worse memory performance. Moreover, this condition was associated with reduced pattern separation and a shift to errors indicative of pattern completion. Based on these findings, we conducted a randomized controlled trial (RCT) of the functional significance of excess fMRI activation and its contribution to cognitive impairment in aMCI subjects, using levetiracetam, an atypical anti-epileptic. We demonstrated that reduction of DG/CA3 BOLD overactivity, resulting from levetiracetam treatment, improved performance of the aMCI subjects on the 3-judgment memory scanning task (Bakker et al., 2012). The full RCT enrolled three cohorts of aMCI patients who were treated with levetiracetam in a range of low doses and evaluated on the 3-judgment memory task designed to assess pattern separation/completion processes. Here we report the findings from the full dose-finding study. The study focused on the network components most affected in the animal models, particularly subregions of the hippocampal formation and the entorhinal cortex. Consistent with those models, we reliably observed elevated fMRI BOLD activation localized to the DG/CA3 subregion of the hippocampal formation, together with a consistent profile in memory performance showing a shift in bias away from pattern separation in favor of pattern completion across aMCI cohorts. At doses of levetiracetam that improved memory performance in the scanning task, drug treatment also normalized fMRI activation in both the entorhinal cortex and DG/CA3 region, reducing DG/CA3 fMRI activity and boosting decreased fMRI activation in the entorhinal cortex (EC). Those findings are consistent with the close coupling across animal and human data in aging and prodromal Alzheimer's disease, with growing interest in the role of neural hyperactivity as a potential therapeutic target to restore the network properties of circuits that are among the earliest affected in Alzheimer's disease (Stargardt et al., 2015).

2. Methods

2.1. Study design

The design for this study is schematically shown in Fig. 1. The entire RCT protocol consisted of 4 study visits over an 8-week period. Each cohort of aMCI participants was randomized, double-blind, in a within-subject crossover design, with the order of treatment on drug and placebo counterbalanced within each cohort. Age-matched controls were treated single-blind on placebo as further described in the procedures that follow.

2.2. Participants and clinical characterization

During the baseline visit all participants completed the dementia rating scale (CDR: Morris, 1993), and underwent medical, psychiatric,

neurological and neuropsychological evaluations, which included the Mini Mental Status Exam (Folstein et al., 1975), the Buschke Selective Reminding Test (Buschke and Fuld, 1974), the Verbal Paired Associated subtest of the Wechsler Memory Scale (Wechsler, 1987) and the Benton Visual Retention Test (Benton, 1974). All aMCI participants had a global CDR score of 0.5 with a sum of boxes score not exceeding 2.5 and met criteria for aMCI proposed by Petersen (Petersen, 2004), which includes impaired memory function on testing and no decline in basic activities of daily living. All control subjects had a global CDR score of 0. None of the aMCI participants or age-matched control subjects met criteria for dementia. Other exclusion criteria included major neurological and psychiatric disorders, head trauma with loss of consciousness, history of substance abuse or dependency, and general contraindications to having an MRI examination (e.g. cardiac pacemaker, aneurysm coils and claustrophobia) or taking the study medication (e.g. known sensitivity or allergies, or severe renal impairment). Participants taking anti-epileptic medications were excluded from participation in the study but use of other neuroactive medications was permitted if the participant was stable on the medication for at least 12 weeks and if the treatment regimen was not altered for the duration of the study. The study protocol was approved by the Institutional Review Board of the Johns Hopkins Medical Institutions. All participants provided written informed consent and were paid for their participation in the study.

At the baseline evaluation sixty-nine participants with aMCI and 24 age-matched controls met criteria for enrollment. Complete data from 54 participants with aMCI and 17 control participants were included in the analysis. Nine aMCI participants and 6 control participants did not complete the study protocol. Data from an additional 6 aMCI participants and 1 control participant were excluded before analysis due to excessive motion or in-scanner task performance that was inadequate for analysis of the fMRI data.

2.3. Study procedures

All participants completed the same study procedures with fMRI study visits after each of two treatment phases, separated by a washout period of 4 weeks as shown in Fig. 1. Control subjects were given placebo during both treatment phases (single-blind) while participants with aMCI were given placebo during one treatment phase and drug during the other treatment phase, with the order of treatment counterbalanced (randomized, double-blind). A first cohort of aMCI participants received treatment with 125 mg BID of levetiracetam (Keppra, UCB Laboratories), as was previously reported (Bakker et al., 2012). Based on those initial findings and earlier preclinical data in animals (Koh et al., 2010), two additional doses were selected for two subsequent cohorts of aMCI participants, receiving treatment with 62.5 mg BID and 250 mg BID of levetiracetam, respectively. All study treatments (drug and placebo)
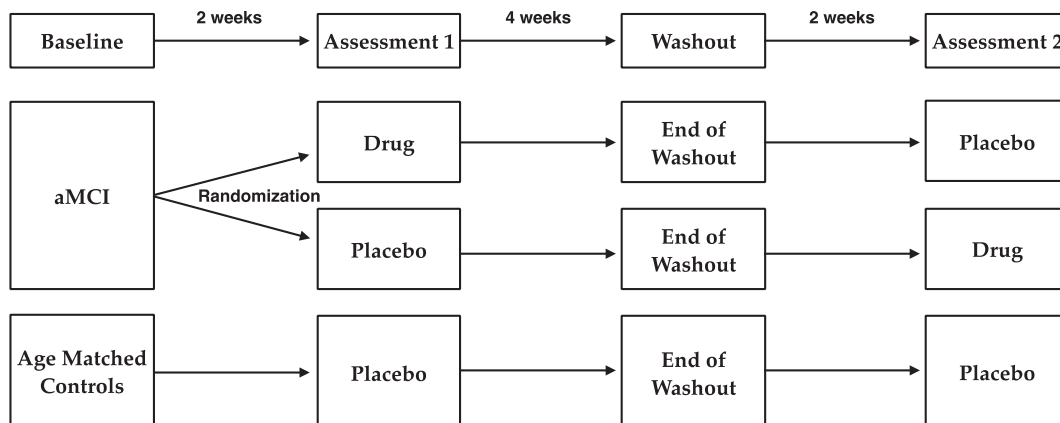

Fig. 1. Schematic of the study design.

were prepared in identical non-descript capsules by the Investigational Drug Service at Johns Hopkins Hospital. Capsules were provided in blister packs labeled for morning and evening daily doses. After 2 weeks on treatment, each study visit included a brief medical and psychiatric examination, the neuropsychological assessment, a blood draw and an MRI scan during performance of the 3-judgment memory task. At the end of the washout visit, each participant had a blood draw and was provided with the study medication for the second treatment phase of the study. Treatment compliance was assessed by participant self-report at the end of each treatment phase, medication diaries, and analysis of levetiracetam blood values at each visit during the study protocol.

The study team was blind to the status of the aMCI participants and levetiracetam blood levels until final group analysis of the data. In addition to providing the study medication the Investigational Drug Service randomized aMCI participants to the treatment conditions and controlled blinding and unblinding of study data according to standard clinical trial procedures. Data safety was monitored by three physicians not related to the study in collaboration with the Investigational Drug Service.

2.4. fMRI activation paradigm

The fMRI activation paradigm was a 3-alternative forced choice task designed to assess pattern separation and completion processes, as mentioned above (Bakker et al., 2012, 2008; Kirwan and Stark, 2007). For this task participants were asked to view a series of stimuli consisting of 768 pictures of common namable objects (see Fig. 2). This included 96 pairs of related but not identical pictures of the same object referred to as lures, 96 pairs in which the identical picture was repeated, referred to as repeats and 384 unrelated single pictures of objects used as foils. Stimuli were divided over eight runs of 96 stimuli per run. Each stimulus was presented for 2500 ms with a 500 ms inter-stimulus-interval consisting of a blank screen. All trials were presented in pseudo-random order with the limitation that a lure or repeated stimulus was presented within 30 trials of its pair. For each stimulus, the participant was asked to judge if the picture was 'new', 'old' or 'similar' but not identical. Stimuli were presented and responses collected using an Apple Macintosh laptop computer running MATLAB software (The Mathworks, Natick, MA), a back-projection screen

and an LCD projector located outside of the scan room. Participants viewed stimuli via a mirror mounted on the head coil. Responses were made using one button in the left hand and two buttons in the right hand connected to a Cedrus RB-610 response box. Before each MRI session subjects completed a brief practice task consisting of 96 trials outside of the scanner to familiarize themselves with the stimuli and the procedures.

2.5. MRI data acquisition

Imaging sessions were conducted on a 3 Tesla Philips scanner (Philips, Eindhoven, The Netherlands) equipped with a SENSE parallel imaging head coil (MRI Devices, Inc., Waukesha) and higher order shims to compensate for local field distortions at the F.M. Kirby Research Center for Functional Brain Imaging at the Kennedy Krieger Institute on the Johns Hopkins Medical Campus. High-resolution functional images were collected using a T2*-weighted echo planar single shot pulse sequence with an acquisition matrix of 64×64, an echo time of 30 ms, a flip angle of 70°, a sense factor of 2, an in plane resolution of 1.5×1.5 mm and a TR of 1.5 s (Kirwan et al., 2007). Each volume consisted of 19 oblique 1.5 mm thick axial slices with no gap oriented along the principal axis of the hippocampus and covered the medial temporal lobe bilaterally. Four dummy scans were completed at the beginning of each run to allow for stabilization of the MR signal. In addition, a whole brain structural scan was acquired using a magnetization prepared rapid gradient echo (MPRAGE) T_1-weighted sequence with 231 oblique slices, 0.65 mm isotropic resolution and a field of view of 240.

2.6. fMRI data analysis

Image data analysis was performed using the Analysis of Functional Neuroimages (AFNI) software package (Cox, 1996). The functional images were first co-registered to correct for slice timing and head motion, using a three-dimensional registration algorithm creating motion vectors to remove trials in which a significant head motion occurred plus and minus one TR from further analysis. Of critical interest were the participants' responses on the 'lure' items used to assess the balance between pattern separation and pattern completion functions in the hippocampal formation. To avoid confusion, throughout the paper we
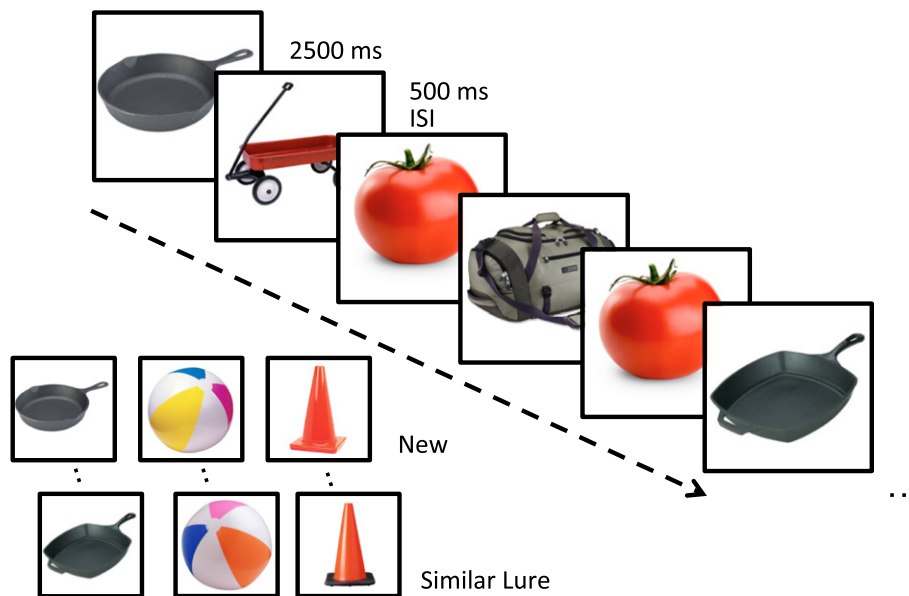

Fig. 2. Task designed to tax hippocampal DG/CA3 function. Participants were shown a series of pictures of every day objects and asked to judge if the item was new (seen for the first time), old (a repeated item) or similar (resembled a previously shown item). The lure items served as the critical trials for assessing performance dependent on the dentate gyrus/CA3.

will refer to items subsequently tested with repetitions as 'subsequent targets' and novel items subsequently tested with a similar lure as 'subsequent lures'. The subsequent items all refer to the 1st presentation trials. During the 2nd presentation, trials will be referred to as targets and lures respectively.

Following this convention, functional runs were concatenated and 6 vectors were defined to model the different trial types: (1) repeats subsequently called "old", (2) lures subsequently called "similar", (3) lures subsequently called "old", (4) repeats called "old", (5) lures called "similar" and (6) lures called "old". All other response types (misses, false alarms, etc.) were modeled but not included in the secondary analyses. The full set of vectors were used to model each individual's data using a deconvolution approach based on general linear regression treating the single foil presentations that were correctly rejected as a non-zero baseline against which all other conditions were compared. The resulting statistical fit coefficient maps represent the difference in activity between each of the trial types and the baseline for a given time point for a given voxel. The sum of the fit coefficients over the length of the hemodynamic response (~3–12 s after the onset of the trial) was taken as the model's estimate of the response to each trial type. The statistical maps were then smoothed using a Gaussian kernel of 3 mm to account for variations in individual functional anatomy.

2.7. Cross-participant alignment

Methods used for cross-participant alignment in this study increase the power of multi-subject regional fMRI studies by focusing the alignment power to the regions of interest using a segmentation of the subject's anatomical image. Initial affine registration was used to transform the subject's anatomical and functional images to the Talairach coordinate system (Talairach and Tournoux, 1988). Subregions of the medial temporal lobe and the hippocampus were manually segmented into three dimensions using the structural scan and methods described previously (Bakker et al., 2008; Kirwan et al., 2007; Yassa and Stark, 2009). Briefly, the entorhinal cortex, perirhinal cortex, parahippocampal cortex, and temporopolar cortices were defined bilaterally in the coronal plane using methods described by Insausti et al. (1998). The CA1, DG/CA3 and subiculum subregions of the hippocampus were also defined in the coronal plane following landmarks described in the atlas of Duvernoy (2005). The DG/CA3 region included the CA2/CA3/CA4 and dentate gyrus subregions as these regions cannot be reliably separated on MRI scans. Using both the segmentation label-based information for the point-set expectation (PSE) error metric and the grayscale structural image for the pure cross-correlation (PR) error metric, Advanced Normalization Tools (ANTs) was used to calculate the 3D vector field transformation for each subject needed to align the individual's ROIs to a template modal model of the ROIs based on the entire sample (Klein et al., 2009; Yushkevich et al., 2009) equally weighing the segmentations and T_1 gray scale data. The 3D vector field for each individual was then applied to the concatenated fit coefficient maps resulting from the functional analysis.

2.8. Statistical analysis

Age, education and neuropsychological and functional assessment scores between groups were compared using independent sample t-tests. The distribution of sex between groups was compared using a chi-square test.

The primary objective of the study was to determine the efficacy of levetiracetam treatment in participants with aMCI, using within-subject comparisons for each cohort. To facilitate a comparison of the fMRI data across the three cohorts of aMCI participants, independent analyses were first conducted for each cohort using a two-way ANOVA with trial type (6 trial type vectors) and group status (aMCI on placebo and aged-matched control group) as fixed factors and subject as a random factor nested within group. A liberal voxel threshold of p < 0.07

was used on the main effect of group F-statistic in combination with a spatial extent threshold of 40 voxels to select areas of task-related activation. The resulting areas of activation were then combined with the anatomical segmentations in order to include only voxels within our areas of interest. The hybrid functional/anatomical analysis resulted in clusters of voxels in each aMCI cohort where activity varied systematically between aMCI and control cohorts within each of the anatomical regions of interest. Voxels within each functional/anatomical region of interest were then collapsed for further analysis. Planned comparisons using t-tests were used for comparisons between the control and the aMCI cohorts on placebo and for the comparisons within each aMCI cohort comparing the aMCI participants on placebo and on levetiracetam on the critical trial type.

3. Results

3.1. Participants

The aMCI participants in each of the treatment cohorts did not significantly differ in age, education and proportion of males and females from the subjects in the control group. Consistent with enrollment criteria, participants with aMCI scored significantly lower on immediate and delayed recall on tests of verbal and visual memory (Table 1).

3.2. Increased DG/CA3 activation and impaired memory task performance in participants with aMCI

In each of the three aMCI cohorts, an area localized in the left DG/CA3 subregion of the hippocampus showed significantly increased BOLD activation during lure trials correctly identified as similar when compared to control subjects (62.5 mg BID, t = 3.074, p = 0.004; 125 mg BID, t = −2.636, p = 0.013 and 250 mg BID, t = 2.070, p = 0.047) (Fig. 3A–C). The aMCI participants in each cohort also had a similar profile in the 3-judgment memory task relative to aged-matched controls as assessed by the rates of each response option (old, similar, or new) on the critical lure trials. For those trials, a between-groups ANOVA revealed a significant effect of response type and, importantly, a significant group by response interaction in each cohort. A post-hoc analysis of that interaction by a planned contrast showed that aMCI participants on placebo incorrectly identified lure items as 'old' more often and gave relatively fewer correct responses of 'similar' compared to control subjects (Control vs. aMCI placebo by Old vs. Similar 62.5 mg BID, F(1,35) = 4.272, p = 0.046; 125 mg BID F(1,32) = 7.687, p = 0.009; 250 mg BID F(1,32) = 9.167, p = 0.005) (Fig. 3A–C). That profile of fewer correct 'similar' responses is consistent with reduced pattern separation and a shift to pattern completion, e.g. more erroneous responses of 'old' in aMCI.

3.3. Levetiracetam treatment reduces DG/CA3 fMRI activation in aMCI and improves memory function

To assess whether low dose levetiracetam treatment effectively reduces hippocampal activation, functional data during the fMRI memory task performance in aMCI participants under placebo treatment was compared with the data from those same participants under levetiracetam treatment. The neuroanatomical regions of altered activity obtained from the initial comparison of aMCI on placebo with the age-matched control group for each of the three treatment cohorts were used to assess the effects of levetiracetam treatment.

At the lowest dose, levetiracetam treatment using 62.5 mg BID did not significantly reduce BOLD activation compared to the placebo condition (t = 1.417, p = 0.1726) during trials correctly identified as similar. However, activation in the DG/CA3 subregion after levetiracetam treatment with 62.5 mg BID no longer differed from activity in that region observed in the age-matched control group. Levetiracetam treatment using 125 mg BID significantly reduced BOLD activation

Table 1
Demographics and clinical characterization of healthy controls and aMCI participants.

Characteristic	Controls		aMCI 62.5 mg BID			aMCI 125 mg BID			aMCI 250 mg BID		
	Mean	SD	Mean	SD	p-Value	Mean	SD	p-Value	Mean	SD	p-Value
Subjects	17		20		—	17		—	17		—
Sex (M/F)	9/8		9/11		0.719	6/11		0.381	6/11		0.381
Age (years)	69.4	7.0	71.0	6.4	0.476	72.9	8.9	0.201	70.8	7.0	0.542
Education (years)	15.9	2.6	15.3	2.8	0.505	15.8	2.9	0.951	16.8	2.6	0.290
CDR	0		0.5		—	0.5		—	0.5		—
CDR sum of boxes	0.03	0.1	0.88	0.5	—	1.0	0.6	—	1.2	0.6	—
MMSE	27.9	1.5	26.5	2.5	0.048	25.7	2.3	0.002	25.9	2.5	0.007
LM delayed recall	29.5	5.2	17.8	9.4	<0.001	15.4	8.2	<0.001	22.9	7.7	0.006
BSRT delayed recall	7.7	1.9	4.5	2.9	<0.001	3.6	2.4	<0.001	3.4	2.1	<0.001
Wechsler VPA delayed recall	7.0	1.5	4.3	2.6	<0.001	3.9	2.9	<0.001	5.2	2.7	0.026
BVRT	5.8	1.8	4.9	1.6	0.091	4.5	1.5	0.026	5.2	1.7	0.338

CDR: Clinical Dementia Rating; MMSE: Mini Mental Status Exam; LM: Logical Memory Paragraph Recall; BSRT: Buschke Selective Reminding Test; VPA: Verbal Paired Associates; BVRT: Benton Visual Retention Test. p-Values are based on independent sample t-tests comparing each aMCI cohort to the control group.

during the correctly identified lure trials relative to the activity during those trials under placebo treatment (t = 2.279, p = 0.037). Levetiracetam treatment with 250 mg BID did not change activation during lure trials correctly identified as similar relative to the activity during such trials under placebo treatment (t = 0.326, p = 0.749) (Fig. 4A, C and E).

Treatment with low dose levetiracetam also improved behavioral performance on the lure trials in treatment groups where levetiracetam treatment normalized increased DG/CA3 activity. A post-hoc analysis of the interaction by planned contrast showed that relative to their performance on placebo, aMCI participants taking 62.5 mg BID or 125 mg BID of levetiracetam made fewer incorrect responses of 'old' while concomitantly increasing correct judgments of 'similar' (aMCI drug vs. aMCI placebo by Old vs. Similar; 62.5 mg BID F(1,19) = 4.783, p = 0.041; 125 mg BID F(1,16) = 5.028, p = 0.039) and performance under drug treatment in these groups were no longer significantly different from healthy control subjects (aMCI drug vs. Control by Old vs. Similar; 62.5 mg BID F(1,35) = 1.823, p = 0.186; 125 mg BID F(1,32) = 1.945, p = 0.173) (Fig. 4B and D). Finally, in addition to not altering activation in the left DG/CA3 during the critical lure trials, treatment with 250 mg BID of levetiracetam also did not improve performance compared to their performance on placebo. Relative to their performance on placebo aMCI participants taking 250 mg BID of levetiracetam did not alter the proportion of old and similar responses to lures (aMCI drug vs. aMCI placebo by Old vs. Similar; F(1,16) = 1.492, p = 0.2396) and remained significantly different from control subjects (aMCI drug vs. Control by Old vs. Similar; F(1,32) = 5.208, p = 0.029) (Fig. 4F).

To confirm the finding that low dose levetiracetam treatment effectively reduces hippocampal activation, a separate analysis was conducted in which voxel selection was based on a one-way ANOVA of trial type only in control subjects. This analysis resulted in an area of task-related activation similarly localized to the left DG/CA3 subregion of the hippocampus. The effect of drug treatment was confirmed by comparing fMRI activation in that area of task-related activity in aMCI participants on placebo and levetiracetam within each of the three aMCI cohorts. Confirming the treatment effects shown in Fig. 4 this analysis similarly showed that levetiracetam treatment using 62.5 mg BID lowered but did not significantly reduce BOLD activation compared to the placebo condition (t = 1.503, p = 0.1492). Levetiracetam treatment using 125 mg BID significantly reduced BOLD activation during the correctly

identified lure trials relative to the activity during those trials under placebo treatment (t = 2.192, p = 0.044). Levetiracetam treatment with 250 mg BID, in contrast, showed no evidence of reducing activation (t = 0.1773, p = 0.8615).

3.4. Levetiracetam treatment normalizes fMRI activation in the entorhinal cortex in aMCI participants

In addition to areas of task related activity in the DG/CA3, analyses of the functional imaging data also revealed an area of *reduced* task related activity in the left entorhinal cortex (EC) in both the 62.5 mg BID cohort and the 125 mg BID cohort. In the left entorhinal cortex, participants with aMCI on placebo showed significantly decreased BOLD activation during those same lure trials compared to control subjects (62.5 mg BID, t = 3.443, p = 0.002 and 125 mg BID, t = 3.278, p = 0.003). After drug treatment BOLD activation in the left EC was increased and normalized in aMCI participants during the critical lure trials in comparison to placebo treatment. This increase was statistically significant in the 62.5 mg BID cohort (t = 3.318, p = 0.004) but not statistically significant in the 125 mg BID cohort (t = −1.60, p = 0.129). In both cohorts activity in the left EC after drug treatment was no longer different from activity observed in the left EC in control subjects (Fig. 5).

3.5. Levetiracetam blood levels

These effects on BOLD activation in the left DG/CA3 and EC in the 62.5 mg BID and 125 mg BID treatment cohorts were obtained with drug doses well below those used clinically for the treatment of epilepsy. Drug levels in aMCI patients were determined to be 2.9 ± 0.29 μg/mL (mean ± SEM) for the 62.5 mg BID cohort and 4.4 ± 0.53 μg/mL for the 125 mg BID cohort. The ineffective dose of 250 mg BID provided a drug level of 7.91 ± 0.92 μg/mL. These levels of drug exposure are well below typical ranges for efficacy of levetiracetam as an anti-epileptic agent where doses of 1000–3000 mg/day are typical, achieving levels of 10–40 μg/mL (Lyseng-Williamson, 2011).

Consistent with Bakker et al. (2012) measures of standard neuropsychological test performance were not affected in any of the three treatment cohorts.

Fig. 3. Increased hippocampal DG/CA3 activation is observed in the context of impaired memory performance in three aMCI cohorts. Task related activation and behavioral performance during the placebo condition in participants with aMCI in the (A) 62.5 mg BID treatment group, (B) 125 mg BID treatment group and (C) 250 mg BID treatment group. (A–C) Top left in A–C: sagittal view of the left medial temporal lobe. Green vertical lines identify slices through the hippocampus shown to the right. Top middle in A–C: segmentation of the structures of interest including the CA1, dentate gyrus/CA3 (DG/CA3), and subiculum (SUB) subregions of the hippocampus. Top right in A–C: coronal slices show statistical maps of the extent of task related activity in the left DG/CA3 from anterior to posterior. Bottom left in A–C: mean activity during lure trials correctly called similar. Participants with aMCI on placebo in each of the treatment groups show increased activity in the left DG/CA3 compared to healthy control subjects during lure trials based on independent samples t-tests. Bottom right in A–C: participants with aMCI on placebo in each of the treatment groups show impaired memory performance by more often incorrectly judging lure items as "old" instead of similar when compared to healthy control subjects. Statistics show p-values resulting from a planned post-hoc contrast for the interaction of group as a function of response type (old versus similar). Values are means ± SEM. *p < 0.05.
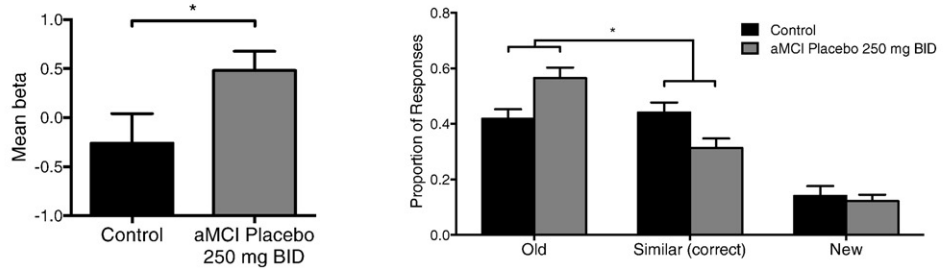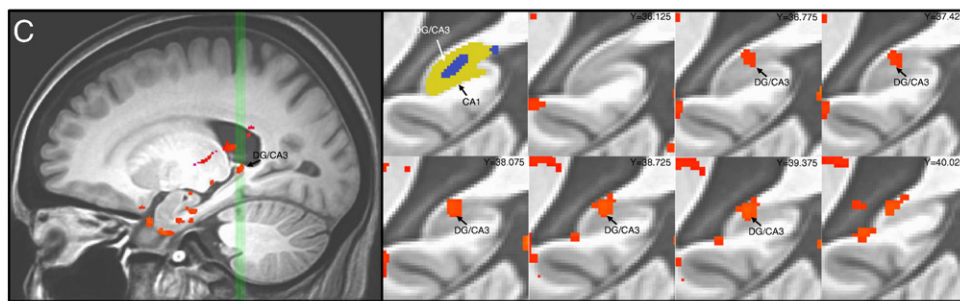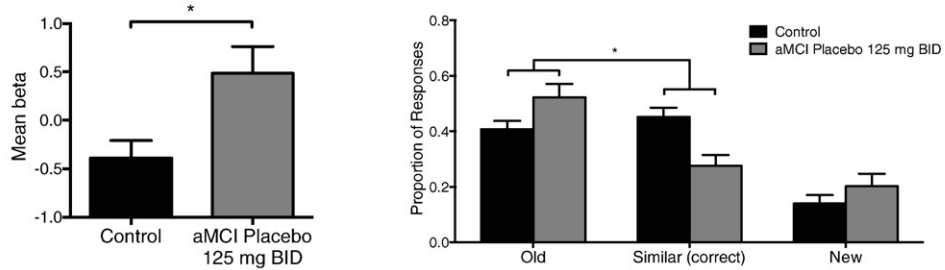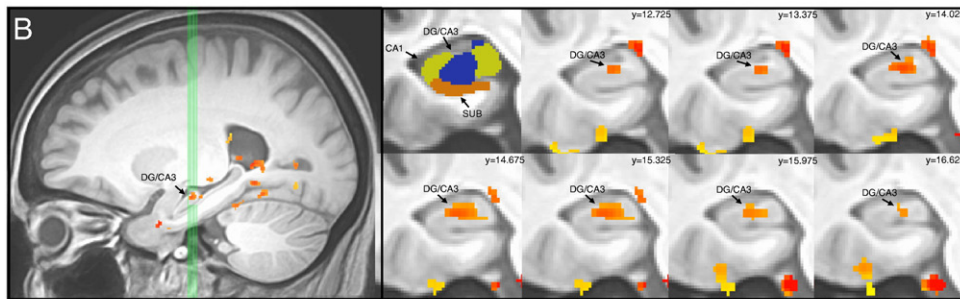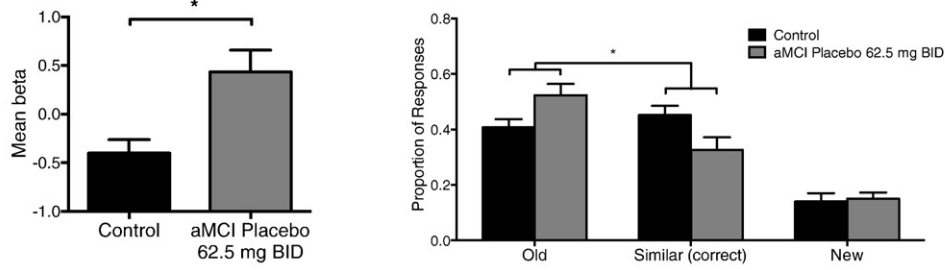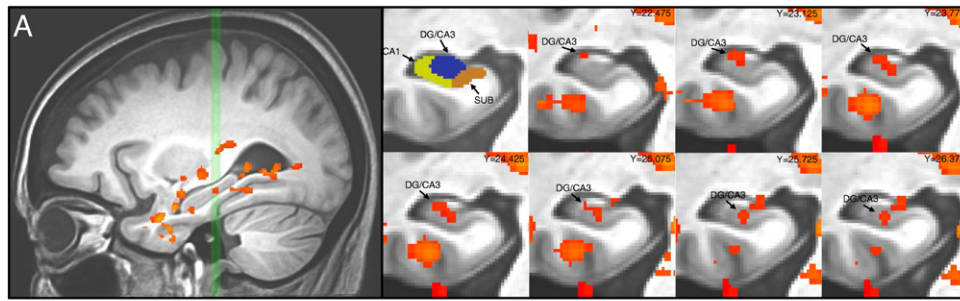
4. Discussion

The primary focus in the current study was to assess the effects of treatment with the atypical anti-epileptic, levetiracetam, on memory performance in the scanning task and fMRI signals in aMCI patients. In the current investigation, low doses of levetiracetam (62.5 and 125 mg BID) significantly improved memory performance in the scanning task with attenuation of overactivity, an effect that was statistically significant at 125 mg BID. In contrast, no difference in either memory task performance or fMRI activation was observed at 250 mg BID. The current findings further suggest that in the dose range of 62.5–125 mg BID, levetiracetam confers benefit on the network properties of the medial temporal lobe memory system. In addition to excess fMRI activation, a region of decreased activation in the entorhinal cortex (EC) was observed during task performance, similar to Yassa et al. (2010). While overactivity was attenuated by levetiracetam in aMCI cohorts treated with low doses (62.5 and 125 mg BID), decreased EC activation was concurrently normalized, with a significant boost in EC activation at the 62.5 mg BID dose compared to placebo.

The observed areas of fMRI activation, consistently localized to the left DG/CA3 subregion in aMCI patients relative to age-matched controls, differed somewhat across cohorts in an anterior to posterior location. Although differences in anterior–posterior localization have been observed in neuroimaging studies using a variety of task-activated fMRI paradigms, the functional significance of such localization remains somewhat equivocal (see Poppenk et al., 2013 for review). Of possible relevance in the current context Malykhin et al. (2010) noted a relatively greater proportion of CA fields (CA1-3) in the anterior hippocampal formation with the DG having a proportionately greater representation at the posterior segments of the long axis. Overactivity in areas of activation localized anterior to posterior, as reported here and elsewhere (Bakker et al., 2012; Yassa et al., 2010) in the context of the 3-judgment recognition task could reflect a relatively greater contribution of augmented pattern completion in anterior areas of activation with any excess activation reflecting a loss of pattern separation in DG contributing more in posterior areas of activation. Overall, however, these findings suggest that excess fMRI activation in the DG/CA3 is associated with a consistent profile of memory task impairment across all three aMCI cohorts.

Importantly, no evidence was found in this study to support a beneficial compensatory role in cognition for excess hippocampal activation. Instead, the data support the view that hippocampal overactivity contributes to symptomatic impairment in the MCI phase of disease (for review see Ewers et al., 2011). Because MCI patients with hippocampal overactivation also exhibit greater cortical thinning, which is indicative of early Alzheimer's disease (AD) related neurodegeneration (Putcha et al., 2011), and excess hippocampal activation detected by fMRI predicts subsequent cognitive decline (Miller et al., 2008), it is hypothesized that hippocampal overactivity contributes to disease progression and neuronal damage if not controlled.

The deleterious effect of hippocampal overactivity detected by fMRI is further supported by recent evidence of a distinctive gene expression profile underlying excessive hippocampal excitability in MCI patients. In a study of autopsy brain samples, Berchtold et al. (2014) reported that the mRNA microarrays from MCI brains exhibited a profile that clustered those patients together and segregated them from groups of older controls and patients with a diagnosis of Alzheimer's dementia. In addition, mRNA markers for hippocampal excess excitability and aberrant plasticity, which were hallmarks in the MCI profile, were correlated with severity of cognitive impairment within the MCI cohort. The reliable signature of hippocampal overactivity in the current study for three cohorts of aMCI patients aligns with such data, as does the detection of overactivity in the CA3/DG subregion reported in a separate study of aMCI patients (Yassa et al., 2010).

Studies using neural recordings in rats first focused attention on the computational functions of the DG and CA3 regions as a basis for age-related memory impairment. Such studies in aged rats with memory impairment have demonstrated a computational shift away from pattern separation in the encoding properties of hippocampal neurons; instead of the rapid encoding of new information, neurons retrieve a previously encoded representation (Wilson et al., 2006, 2003). Likewise in studies comparing young vs. older adults, the use of lures that are similar, but not identical, in 3-judgment recognition demonstrates that elderly participants make fewer correct responses of 'similar' indicative of pattern separation, while increasing errors that reflect pattern completion, e.g. judging lure items as 'old' repeats (Lacy et al., 2011; Stark et al., 2013; Toner et al., 2009; Yassa et al., 2011b). Patients with aMCI have shown further worsening in memory impairment on lure items compared to age-matched controls (Stark et al., 2013; Yassa et al., 2011b), as observed in the current investigation. Increased fMRI activation in the DG/CA3 subregion in human aging (O'Brien et al., 2010; Yassa et al., 2011a) and its further augmentation in aMCI, as reported here and elsewhere (Bakker et al., 2012; Yassa et al., 2010), may primarily reflect an elevation of CA3 neural activity which has been directly observed in memory-impaired aged rats (Wilson et al., 2005). Overactive CA3 neurons and their massive recurrent collaterals are a likely a basis for driving greater pattern completion to shift the balance away from pattern separation.

Although it is not possible to reliably differentiate DG apart from CA3 in human brain imaging, any greater activation in the DG contributing to the elevated fMRI signal in composite DG/CA3 areas of activation could also reflect diminished pattern separation in the DG itself. In addition to elevated activity in the firing rates of CA3 pyramidal neurons, another distinctive signature of aged memory-impaired rats is a loss of integrity affecting the interneurons in the hilus (Spiegel et al., 2013), which normally limits the activation of granule cells receiving perforant path input from the EC (Andrews-Zwilling et al., 2010). In a mouse model of genetic risk for Alzheimer's disease, ApoE4 has been observed to augment the age-dependent loss of hilar interneuron integrity further reducing inhibitory control of DG granule cells (Andrews-Zwilling et al., 2010). Although somewhat speculative, if a similar condition occurs in humans, a greater number of granule cells activated by perforant path input could contribute to elevated fMRI activation in DG/CA3 reflecting degradation of the sparse encoding by granule cells, a property that is critical for pattern separation.

With respect to the EC, the current findings of decreased fMRI activation replicate that condition previously reported in aMCI patients compared to age-matched controls (Yassa et al., 2010). Studies with animal models have pointed to the EC as contributing to age-related memory impairment and studies with humans have confirmed the progressive worsening of that impairment in patients with aMCI. Notably, in rats the presence and severity of cognitive impairment in aging are tightly coupled to loss of synaptic integrity for the layer 2 neurons in the EC innervating DG and CA3 (Smith et al., 2000). In humans a further loss of those connections is observed in MCI and AD compared to aging, with that synaptic loss correlating with worse delayed-recall memory performance (Scheff et al., 2006). Additionally, molecular alterations affecting the EC layer 2 neurons occur in both age-related memory impairment in rodents (Stranahan et al., 2011), as well as in AD animal models (hAPP mice) and AD patients (Chin et al., 2007). Thus the network comprised of the EC together with the hippocampal formation exhibits features underlying age-related cognitive impairment that exhibits a further progression in aMCI compared to aging. It should be noted, however, that the current methods for detection of decreased fMRI activation in the EC were not localized to a specific EC layer. The fMRI signature in aMCI and its restoration by treatment could be due to beneficial effects on the network overall, involving not only EC input to the hippocampus but also hippocampal output to the EC, which innervates deeper EC layers. The relationship between loss of EC input to the DG/CA3 and overactivity in those regions is also not yet clearly defined but could involve the extensive network of
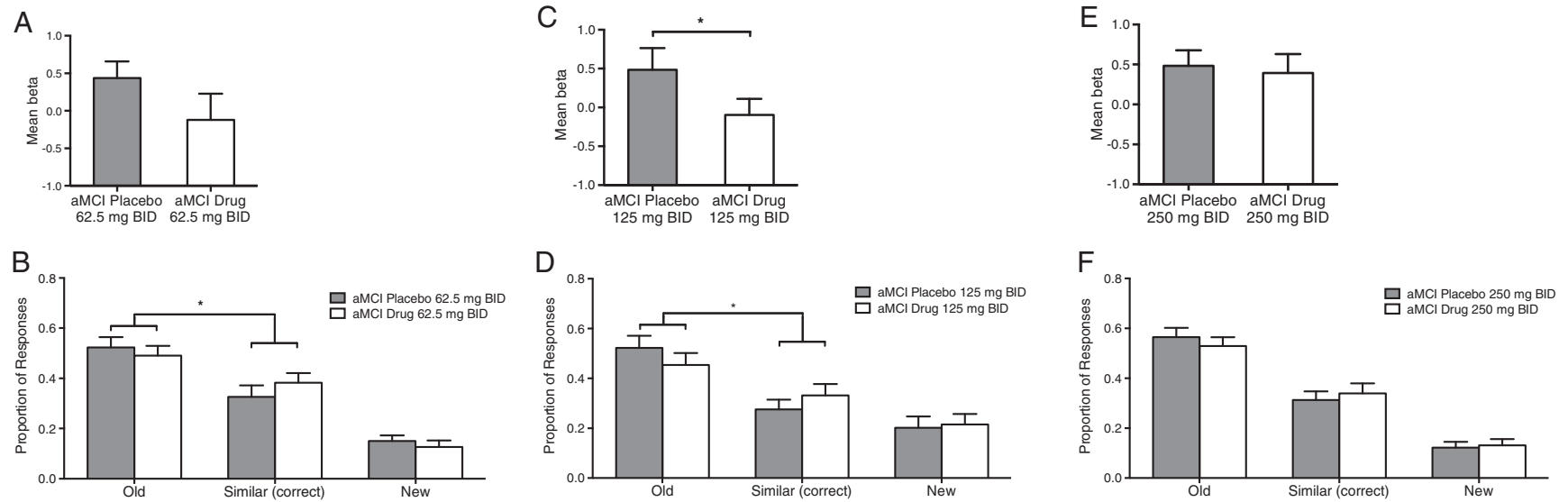
Fig. 4. Low dose levetiracetam normalizes DG/CA3 activation and improves task-related memory performance on critical lure items in participants with aMCI. Top graphs show mean fMRI activity during lure trials correctly called similar. Bottom graphs show behavioral performance as the proportion of lure trials called "old", "new" and "similar". For each cohort all analyses were within-subject comparing placebo with drug treatment. (A) In the 62.5 mg BID cohort levetiracetam did not significantly reduce activity in the DG/CA3 in participants with aMCI although activity under drug treatment was no longer significantly different from healthy control subjects. (B) In the 62.5 mg BID cohort levetiracetam improved memory performance in aMCI participants by reducing errors in which lures were incorrectly judged "old", with more correct judgments of "similar". (C) In the 125 mg BID cohort levetiracetam significantly reduced activation in the DG/CA3 and (D) significantly improved memory performance. (E) In the 250 mg BID cohort treatment levetiracetam did not reduce activity in the DG/CA3 and (F) did not alter memory performance in these patients. Values are means ± SEM. *p < 0.05.
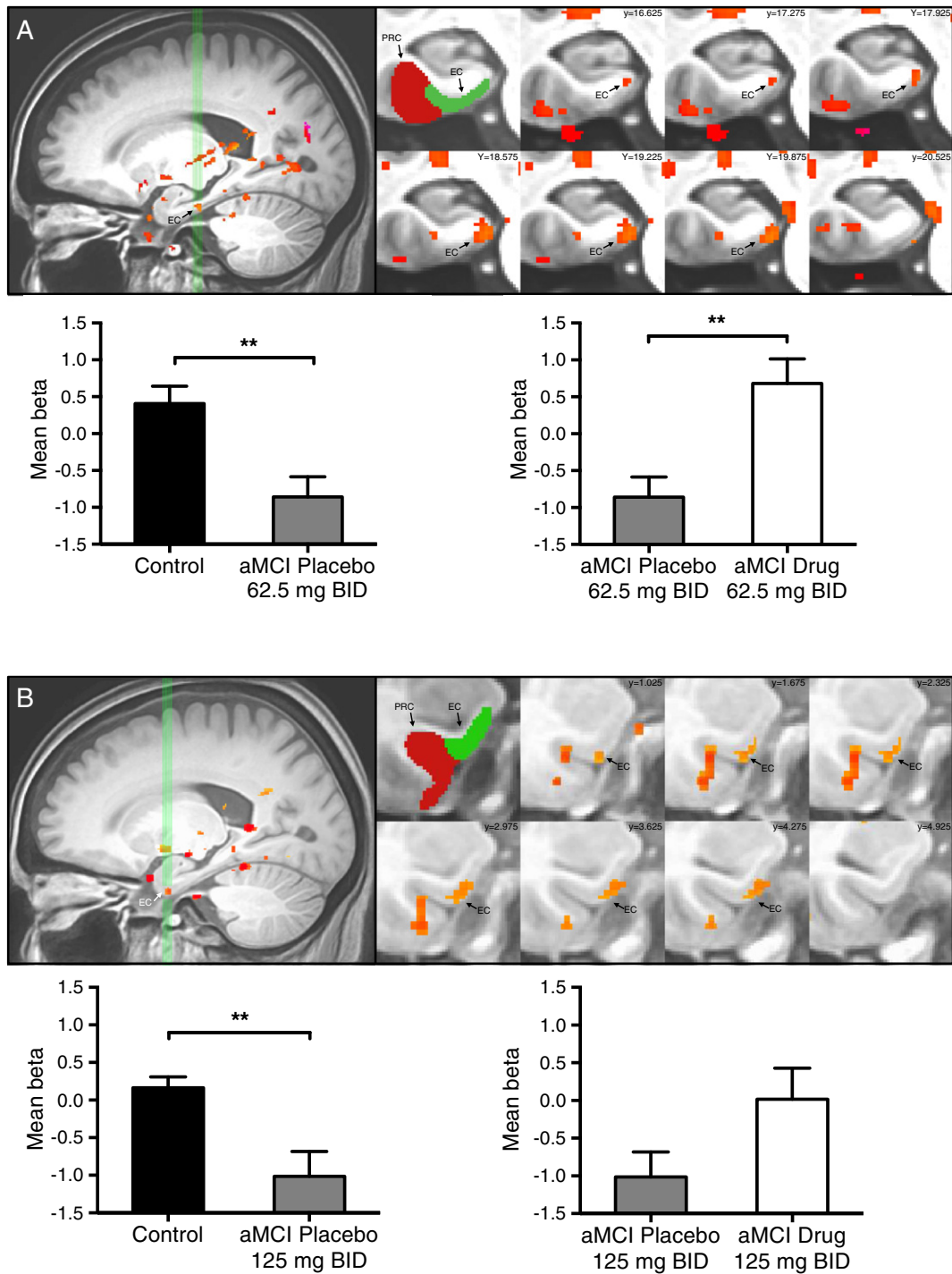
Fig. 5. Low dose levetiracetam normalizes entorhinal cortex activity in participants with aMCI. Task-related activation in (A) 62.5 mg BID treatment group and (B) 125 mg BID treatment group. Top left in A–B: sagittal view of the left medial temporal lobe. Green vertical lines identify slices through the entorhinal cortex shown to the right. Top middle A–B: segmentation of the medial temporal lobe structures including the entorhinal (EC) and perirhinal (PRC) cortices. Top right A–B: coronal slices show statistical maps of the extent of task related activity in the left EC in the 62.5 mg BID treatment cohort and the 125 mg BID treatment cohort.

interneurons that receive EC and DG input to control excitability of principal neurons in the DG/CA3 region.

The current investigation has served to identify a condition detected by brain imaging and its modification by an intervention built on basic research that has increased our understanding of the contribution of circuits involving the EC and its targets in the DG and CA3 regions to memory. The current study leveraged discoveries in cognitive neuroscience based on recordings of the encoding properties of neurons and use of other methods not possible in humans. Studies in rodents, both young adults and in a well-characterized model of neurocognitive aging, were especially informative about the properties of the network underlying age-related memory impairment and initial preclinical tests of therapeutic interventions (Koh et al., 2010, 2013; Wilson et al., 2006). Low doses of the atypical anti-epileptic levetiracetam have shown benefit in conditions of age-related memory impairment in rodents and laboratory models relevant to Alzheimer's disease (Koh et al., 2010; Rhinn et al., 2013; Sanchez et al., 2012; Shi et al., 2013; Suberbielle et al., 2013). Levetiracetam has also been reported to have beneficial

effects in circuits throughout the MTL network when treatment improves hippocampal-dependent cognition (Sanchez et al., 2012). Moreover, a therapeutic window for levetiracetam treatment similar to that observed in the current clinical investigation has also been reported in animal models (Koh et al., 2010; Sanchez et al., 2012; Shi et al., 2013), with a lack of efficacy for levetiracetam dosing in the usual clinical range for treating patients with epilepsy (Koh et al., 2010; Sanchez et al., 2012). Based on such findings, a translation from animal models to humans with the use of brain imaging represents a promising approach to advance discovery in clinical research.

The findings presented here result from a high-resolution approach to defining hippocampal subregions by imaging the medial temporal lobe (MTL). As such the methods do not consider broader network changes that have been observed in aging and MCI, for example involving default mode networks in the cortex. Further research, incorporating both MTL high-resolution and whole brain acquisitions in the same study population will make possible the assessment of such changes as well as changes in connectivity with regions of task-related fMRI in the MTL.

Acknowledgments

References

Alme, C.B., Miao, C., Jezek, K., Treves, A., Moser, E.I., Moser, M.-B., 2014. Place cells in the hippocampus: eleven maps for eleven rooms. Proc. Natl. Acad. Sci. U. S. A. 111 (52), 18428–18435. http://dx.doi.org/10.1073/pnas.142105611125489089.

Andrews-Zwilling, Y., Bien-Ly, N., Xu, Q., Li, G., Bernardo, A., Yoon, S.Y., Zwilling, D., Yan, T.X., Chen, L., Huang, Y., 2010. Apolipoprotein E4 causes age- and Tau-dependent impairment of GABAergic interneurons, leading to learning and memory deficits in mice. J. Neurosci. 30 (41), 13707–13717. http://dx.doi.org/10.1523/JNEUROSCI.4040-10.201020943911.

Bakker, A., Kirwan, C.B., Miller, M., Stark, C.E., 2008. Pattern separation in the human hippocampal CA3 and dentate gyrus. Science 319 (5870), 1640–1642. http://dx.doi.org/10.1126/science.115288218356518.

Bakker, A., Krauss, G.L., Albert, M.S., Speck, C.L., Jones, L.R., Stark, C.E., Yassa, M.A., Bassett, S.S., Shelton, A.L., Gallagher, M., 2012. Reduction of hippocampal hyperactivity improves cognition in amnestic mild cognitive impairment. Neuron 74 (3), 467–474. http://dx.doi.org/10.1016/j.neuron.2012.03.02322578498.

Benton, A., 1974. The Revised Visual Retention Test. Psychological Corporation, New York.

Berchtold, N.C, Sabbagh, M.N., Beach, T.G., Kim, R.C., Cribbs, D.H., Cotman, C.W., 2014. Brain gene expression patterns differentiate mild cognitive impairment from normal aged and Alzheimer's disease. Neurobiol. Aging 35 (9), 1961–1972. http://dx.doi.org/10.1016/j.neurobiolaging.2014.03.03124786631.

Buschke, H., Fuld, P.A., 1974. Evaluating storage, retention, and retrieval in disordered memory and learning. Neurology 24 (11), 1019–1025. http://dx.doi.org/10.1212/WNL.24.11.10194473151.

Chin, J., Massaro, C.M., Palop, J.J., Thwin, M.T., Yu, G.-Q., Bien-Ly, N., Bender, A., Mucke, L., 2007. Reelin depletion in the entorhinal cortex of human amyloid precursor protein transgenic mice and humans with Alzheimer's disease. J. Neurosci. 27 (11), 2727–2733. http://dx.doi.org/10.1523/JNEUROSCI.3758-06.200717360894.

Cox, R.W., 1996. AFNI: software for analysis and visualization of functional magnetic resonance neuroimages. Comput. Biomed. Res. 29 (3), 162–173. http://dx.doi.org/10.1006/cbmr.1996.00148812068.

Duvernoy, H., 2005. The Human Hippocampus: Functional Anatomy, Vascularization, and Serial Sections with MRI. Springer Verlag.

Folstein, M.F., Folstein, S.E., McHugh, P.R., 1975. "Mini-mental state." A practical method for grading the cognitive state of patients for the clinician. J. Psychiatr. Res. 12 (3), 189–198. http://dx.doi.org/10.1016/0022-3956(75)90026-61202204.

Insausti, R., Juottonen, K., Soininen, H., Insausti, A.M., Partanen, K., Vainio, P., Laakso, M.P., Pitkänen, A., 1998. MR volumetric analysis of the human entorhinal, perirhinal, and temporopolar cortices. A.J.N.R. Am. J. Neuroradiol. 19 (4), 659–6719576651.

Kirwan, C.B., Jones, C.K., Miller, M.I., Stark, C.E., 2007. High-resolution fMRI investigation of the medial temporal lobe. Hum. Brain Mapp. 28 (10), 959–966. http://dx.doi.org/10.1002/hbm.2033117133381.

Kirwan, C.B., Stark, C.E., 2007. Overcoming interference: an fMRI investigation of pattern separation in the medial temporal lobe. Learn. Mem. 14 (9), 625–633. http://dx.doi.org/10.1101/lm.66350717848502.

Klein, A., Andersson, J., Ardekani, B.A., Ashburner, J., Avants, B., Chiang, M.-C., Christensen, G.E., Collins, D.L., Gee, J., Hellier, P., Song, J.H., Jenkinson, M., Lepage, C., Rueckert, D.,

Thompson, P., Vercauteren, T., Woods, R.P., Mann, J.J., Parsey, R.V., 2009. Evaluation of 14 nonlinear deformation algorithms applied to human brain MRI registration. Neuroimage 46 (3), 786–802. http://dx.doi.org/10.1016/j.neuroimage.2008.12.03719195496.

Koh, M.T., Haberman, R.P., Foti, S., McCown, T.J., Gallagher, M., 2010. Treatment strategies targeting excess hippocampal activity benefit aged rats with cognitive impairment. Neuropsychopharmacology 35 (4), 1016–1025. http://dx.doi.org/10.1038/npp.2009.20720032967.

Koh, M.T., Rosenzweig-Lipson, S., Gallagher, M., 2013. Selective GABA(A) α5 positive allosteric modulators improve cognitive function in aged rats with memory impairment. Neuropharmacology 64, 145–152. http://dx.doi.org/10.1016/j.neuropharm.2012.06.02322732440.

Lacy, J.W., Yassa, M.A., Stark, S.M., Muftuler, L.T., Stark, C.E., 2011. Distinct pattern separation related transfer functions in human CA3/dentate and CA1 revealed using high-resolution fMRI and variable mnemonic similarity. Learn. Mem. 18 (1), 15–18. http://dx.doi.org/10.1101/lm.197111121164173.

Lee, I., Yoganarasimha, D., Rao, G., Knierim, J.J., 2004. Comparison of population coherence of place cells in hippocampal subfields CA1 and CA3. Nature 430 (6998), 456–459. http://dx.doi.org/10.1038/nature0273915229614.

Leutgeb, S., Leutgeb, J.K., Treves, A., Moser, M.-B., Moser, E.I., 2004. Distinct ensemble codes in hippocampal areas CA3 and CA1. Science 305 (5688), 1295–1298. http://dx.doi.org/10.1126/science.110026515272123.

Lyseng-Williamson, K.A., 2011. Levetiracetam: a review of its use in epilepsy. Drugs 71 (4), 489–514. http://dx.doi.org/10.2165/11204490-000000000-0000021359360.

Malykhin, N.V., Lebel, R.M., Coupland, N.J., Wilman, A.H., Carter, R., 2010. In vivo quantification of hippocampal subfields using 4.7 T fast spin echo imaging. Neuroimage 49 (2), 1224–1230. http://dx.doi.org/10.1016/j.neuroimage.2009.09.04219786104.

McClelland, J.L., McNaughton, B.L., O'Reilly, R.C., 1995. Why there are complementary learning systems in the hippocampus and neocortex: insights from the successes and failures of connectionist models of learning and memory. Psychol. Rev. 102 (3), 419–457. http://dx.doi.org/10.1037/0033-295X.102.3.4197624455.

Miller, S.L., Fenstermacher, E., Bates, J., Blacker, D., Sperling, R.A., Dickerson, B.C., 2008. Hippocampal activation in adults with mild cognitive impairment predicts subsequent cognitive decline. J. Neurol. Neurosurg. Psychiatr. 79 (6), 630–635. http://dx.doi.org/10.1136/jnnp.2007.12414917846109.

Morris, J.C., 1993. The Clinical Dementia Rating (CDR): current version and scoring rules. Neurology 43 (11), 2412–2414. http://dx.doi.org/10.1212/WNL.43.11.2412-a8232972.

Neunuebel, J.P., Knierim, J.J., 2014. CA3 retrieves coherent representations from degraded input: direct evidence for CA3 pattern completion and dentate gyrus pattern separation. Neuron 81 (2), 416–427. http://dx.doi.org/10.1016/j.neuron.2013.11.01724462102.

Norman, K.A., O'Reilly, R.C., 2003. Modeling hippocampal and neocortical contributions to recognition memory: a complementary-learning-systems approach. Psychol. Rev. 110 (4), 611–646. http://dx.doi.org/10.1037/0033-295X.110.4.61114599236.

O'Brien, J.L., O'Keefe, K.M., LaViolette, P.S., DeLuca, A.N., Blacker, D., Dickerson, B.C., Sperling, R.A., 2010. Longitudinal fMRI in elderly reveals loss of hippocampal activation with clinical decline. Neurology 74 (24), 1969–1976. http://dx.doi.org/10.1212/WNL.0b013e3181e3966e20463288.

O'Reilly, R.C., McClelland, J.L., 1994. Hippocampal conjunctive encoding, storage, and recall: avoiding a trade-off. Hippocampus 4 (6), 661–682. http://dx.doi.org/10.1002/hipo.4500406057704110.

Petersen, R.C., 2004. Mild cognitive impairment as a diagnostic entity. J. Intern. Med. 256 (3), 183–194. http://dx.doi.org/10.1111/j.1365-2796.2004.01388.x15324362.

Poppenk, J., Evensmoen, H.R., Moscovitch, M., Nadel, L., 2013. Long-axis specialization of the human hippocampus. Trends Cogn. Sci. 17 (5), 230–240. http://dx.doi.org/10.1016/j.tics.2013.03.00523597720.

Putcha, D., Brickhouse, M., O'Keefe, K., Sullivan, C., Rentz, D., Marshall, G., Dickerson, B., Sperling, R., 2011. Hippocampal hyperactivation associated with cortical thinning in Alzheimer's disease signature regions in non-demented elderly adults. J. Neurosci. 31 (48), 17680–17688. http://dx.doi.org/10.1523/JNEUROSCI.4740-11.201122131428.

Rhinn, H., Fujita, R., Qiang, L., Cheng, R., Lee, J.H., Abeliovich, A., 2013. Integrative genomics identifies APOE ε4 effectors in Alzheimer's disease. Nature 500 (7460), 45–50. http://dx.doi.org/10.1038/nature1241523883936.

Sanchez, P.E., Zhu, L., Verret, L., Vossel, K.A., Orr, A.G., Cirrito, J.R., Devidze, N., Ho, K., Yu, G.-Q., Palop, J.J., Mucke, L., 2012. Levetiracetam suppresses neuronal network dysfunction and reverses synaptic and cognitive deficits in an Alzheimer's disease model. Proc. Natl. Acad. Sci. U. S. A. 109, E2895–E2903. http://dx.doi.org/10.1073/pnas.112108110922869752.

Scheff, S.W., Price, D.A., Schmitt, F.A., Mufson, E.J., 2006. Hippocampal synaptic loss in early Alzheimer's disease and mild cognitive impairment. Neurobiol. Aging 27 (10), 1372–1384. http://dx.doi.org/10.1016/j.neurobiolaging.2005.09.01216289476.

Shi, J.-Q., Wang, B.-R., Tian, Y.-Y., Xu, J., Gao, L., Zhao, S.-L., Jiang, T., Xie, H.-G., Zhang, Y.-D., 2013. Anti-epileptics topiramate and levetiracetam alleviate behavioral deficits and reduce neuropathology in APPswe/PS1dE9 transgenic mice. C.N.S. Neurosci. Ther. 19 (11), 871–881. http://dx.doi.org/10.1111/cns.1214423889921.

Smith, T.D., Adams, M.M., Gallagher, M., Morrison, J.H., Rapp, P.R., 2000. Circuit-specific alterations in hippocampal synaptophysin immunoreactivity predict spatial learning impairment in aged rats. J. Neurosci. 20 (17), 6587–659310964964.

Spiegel, A.M., Koh, M.T., Vogt, N.M., Rapp, P.R., Gallagher, M., 2013. Hilar interneuron vulnerability distinguishes aged rats with memory impairment. J. Comp. Neurol. 521 (15), 3508–3523. http://dx.doi.org/10.1002/cne.2336723749483.

Stargardt, A., Swaab, D.F., Bossers, K., 2015. The storm before the quiet: neuronal hyperactivity and Aβ in the presymptomatic stages of Alzheimer's disease. Neurobiol. Aging 36 (1), 1–11. http://dx.doi.org/10.1016/j.neurobiolaging.2014.08.01425444609.

Stark, S.M., Yassa, M.A., Lacy, J.W., Stark, C.E., 2013. A task to assess behavioral pattern separation (BPS) in humans: data from healthy aging and mild cognitive

impairment. Neuropsychologia 51 (12), 2442–2449. http://dx.doi.org/10.1016/j.neuropsychologia.2012.12.01423313292.

Stranahan, A.M., Haberman, R.P., Gallagher, M., 2011. Cognitive decline is associated with reduced reelin expression in the entorhinal cortex of aged rats. Cereb. Cortex 21 (2), 392–400. http://dx.doi.org/10.1093/cercor/bhq10620538740.

Suberbielle, E., Sanchez, P.E., Kravitz, A.V., Wang, X., Ho, K., Eilertson, K., Devidze, N., Kreitzer, A.C., Mucke, L., 2013. Physiologic brain activity causes DNA double-strand breaks in neurons, with exacerbation by amyloid-β. Nat. Neurosci. 16 (5), 613–621. http://dx.doi.org/10.1038/nn.335623525040.

Talairach, J., Tournoux, P., 1988. Co-planar Stereotaxic Atlas of the Human Brain: 3 Dimensional Proportional System: An Approach to Cerebral Imaging. Thieme.

Toner, C.K., Pirogovsky, E., Kirwan, C.B., Gilbert, P.E., 2009. Visual object pattern separation deficits in nondemented older adults. Learn. Mem. 16 (5), 338–342. http://dx.doi.org/10.1101/lm.131510919403797.

Treves, A., Rolls, E.T., 1994. Computational analysis of the role of the hippocampus in memory. Hippocampus 4 (3), 374–391. http://dx.doi.org/10.1002/hipo.4500403197842058.

Wechsler, D., 1987. WMS-R: Wechsler Memory Scale —Revised Manual.

Wilson, I.A., Gallagher, M., Eichenbaum, H., Tanila, H., 2006. Neurocognitive aging: prior memories hinder new hippocampal encoding. Trends Neurosci. 29 (12), 662–670. http://dx.doi.org/10.1016/j.tins.2006.10.00217046075.

Wilson, I.A., Ikonen, S., Gallagher, M., Eichenbaum, H., Tanila, H., 2005. Age-associated alterations of hippocampal place cells are subregion specific. J. Neurosci. 25 (29), 6877–6886. http://dx.doi.org/10.1523/JNEUROSCI.1744-05.200516033897.

Wilson, I.A., Ikonen, S., McMahan, R.W., Gallagher, M., Eichenbaum, H., Tanila, H., 2003. Place cell rigidity correlates with impaired spatial learning in aged rats. Neurobiol. Aging 24 (2), 297–305. http://dx.doi.org/10.1016/S0197-4580(02)00080-512498963.

Yassa, M.A., Lacy, J.W., Stark, S.M., Albert, M.S., Gallagher, M., Stark, C.E., 2011a. Pattern separation deficits associated with increased hippocampal CA3 and dentate gyrus activity in nondemented older adults. Hippocampus 21, 968–979. http://dx.doi.org/10.1002/hipo.2080820865732.

Yassa, M.A., Mattfeld, A.T., Stark, S.M., Stark, C.E., 2011b. Age-related memory deficits linked to circuit-specific disruptions in the hippocampus. Proc. Natl. Acad. Sci. U. S. A. 108 (21), 8873–8878. http://dx.doi.org/10.1073/pnas.110156710821555581.

Yassa, M.A., Stark, C.E., 2009. A quantitative evaluation of cross-participant registration techniques for MRI studies of the medial temporal lobe. Neuroimage 44 (2), 319–327. http://dx.doi.org/10.1016/j.neuroimage.2008.09.01618929669.

Yassa, M.A., Stark, C.E., 2011. Pattern separation in the hippocampus. Trends Neurosci. 34, 515–525. http://dx.doi.org/10.1016/j.tins.2011.06.00621788086.

Yassa, M.A., Stark, S.M., Bakker, A., Albert, M.S., Gallagher, M., Stark, C.E., 2010. High-resolution structural and functional MRI of hippocampal CA3 and dentate gyrus in patients with amnestic mild cognitive impairment. Neuroimage 51 (3), 1242–1252. http://dx.doi.org/10.1016/j.neuroimage.2010.03.04020338246.

Yushkevich, P.A., Avants, B.B., Pluta, J., Das, S., Minkoff, D., Mechanic-Hamilton, D., Glynn, S., Pickup, S., Liu, W., Gee, J.C., Grossman, M., Detre, J.A., 2009. A high-resolution computational atlas of the human hippocampus from postmortem magnetic resonance imaging at 9.4 T. Neuroimage 44 (2), 385–398. http://dx.doi.org/10.1016/j.neuroimage.2008.08.04218840532.